Hindawi
Shock and Vibration
Volume 2019, Article ID 6073828, 12 pages
https://doi.org/10.1155/2019/6073828

Research Article

Disassembling-Based Structural Damage Detection Using Static Measurement Data

Eun-Taik Lee[1] and Hee-Chang Eun[2]

[1]*Department of Architectural Engineering, Chung-Ang University, Seoul, Republic of Korea*
[2]*Department of Architectural Engineering, Kangwon National University, Chuncheon, Republic of Korea*

Correspondence should be addressed to Hee-Chang Eun; heechang@kangwon.ac.kr

Received 19 April 2019; Revised 14 July 2019; Accepted 10 October 2019; Published 31 October 2019

Guest Editor: Franco Concli

Damage detection methods can be classified into global and local approaches depending on the division of measurement locations in a structure. The former utilizes measurement data at all degrees of freedom (DOFs) for structural damage detection, while the latter utilizes data of members and substructures at a few DOFs. This paper presents a local method to detect damages by disassembling an entire structure into members. The constraint forces acting at the measured DOFs of the disassembled elements at the damaged state, and their internal stresses, are predicted. The proposed method detects locally damaged members of the entire structure by comparing the stress variations before and after damage. The static local damage can be explicitly detected when it is positioned along the constraint load paths. The validity of the proposed method is illustrated through the damage detection of two truss structures, and the disassembling (i.e., local) and global approaches are compared using numerical examples. The numerical applications consider the noise effect and single and multiple damage cases, including vertical, diagonal, and chord members of truss structures.

1. Introduction

The structural performance of members and connections in a structure can deteriorate owing to natural or artificial disasters or careless maintenance during the service period. Structural durability can be improved by carrying out regular inspections, and repairing and strengthening determined damaged locations. The evaluation of the structural performance and detection of damage locations or elements have been extensively researched for decades. With the advent of high-tech measurement sensors and technologies, research in this field has rapidly increased. A nondestructive test using these techniques provides more common and reliable results to diagnose the structural performance.

Damage detection methods can be largely divided into dynamic and static approaches depending on the collected data types. The former method utilizes dynamic responses, while the latter utilizes static responses. The results of the dynamic and static responses are utilized as basic data to detect the location and severity of damage in a structure. The dynamic damage detection method begins with measuring the modal characteristics of dynamic systems using sensors. If the sensitivity of the damage is low, it cannot be explicitly observed. The static approach has attracted considerable attention because accurate response data, such as displacements and strains, can be easily collected. However, Chen et al. [1] indicated the difficulties that the static method needs to overcome. (1) The static method cannot obtain more explicit information than the dynamic approach. (2) The effect of the damage depends on the loading paths, and the static method has limits in detecting the local damage.

The locally damaged elements in an entire structure can be detected by disassembling it into elements and evaluating their performance by elements. Doebling et al. [2] proposed the local stiffness identification method from the elemental stiffness matrix eigenvalues by using a presumed connectivity and a strain energy distribution pattern. Computing a minimum-rank solution for the perturbation of the elemental

stiffness parameters and using the constraint conditions of the connectivity of the global stiffness matrix, Doebling [3] introduced an update method. Disassembling the structural stiffness matrix and estimating the full dynamic residuals using the columns of a spring connectivity matrix, James et al. [4] provided a coupled approach for structural damage detection. Utilizing strain change based on the flexibility index between undamaged and damaged states, Montazer and Seyedpoor [5] provided a damage detection method for truss structures. Bakhtiari-Nejad et al. [6] provided a static damage detection algorithm, utilizing an optimality criterion for minimizing the difference between the load vectors in the damaged and undamaged states. Maity and Saha [7] detected damage using a neural network to recognize the behavior of the undamaged structures and that of the structure with various possible damaged states. Rezaiee-Pajand et al. [8] presented a static damage detection algorithm for frame structures using nonlinear constrained structural optimization. They minimized the difference between the measured and analytical static displacements. Rahmatalla et al. [9] proposed a damage detection method from the distribution of constraint forces in the satisfaction of measured data. Yang [10] proposed a structural damage detection method using the matrix disassembly technique and modal residual force criteria. Yang and Sun [11] proposed a static detection method using the flexibility disassembly technique. Hejelmstad and Shin [12] proposed a static damage detection and assessment algorithm using a data perturbation scheme.

Model-based damage detection methods require the measurement data to evaluate structural health state. These methods can be classified into global and local approaches. In the global approach, the measurement data at all DOFs are utilized simultaneously for damage detection. In the disassembling-based or local approach, the measurement data are disassembled by parts or elements and the local damage is detected.

This study aims to detect the damaged elements along the load path of constraint forces to cause the largest stress variation in all admissible load paths. This paper presents the disassembling-based damage detection method using static responses at the measured DOFs and the corresponding constraint forces. The existence of damage affects the responses of the entire structure. The measured displacements are utilized as constraints to describe the static behavior in the damaged state. The damage can be explicitly detected when it is positioned along the constraint load paths. The validity of the proposed method is illustrated through the damage detection of two truss structures, and the disassembling-based and global approaches are compared using numerical examples. The numerical applications consider the noise effect and single and multiple damage cases, including vertical, diagonal, and chord members in truss structures.

2. Formulation

The initial static responses of a finite-element model do not coincide with those in the damaged state. The variation can be described by the action of an additional force set estimated at the measurement nodes.

A local damage in a structure or member affects the displacement responses at the other locations owing to the structural continuity, because the responses at the damaged element can be described by the action of an external force. The displacement variations at a full set of DOFs can be similarly described by superposing the corresponding constraint force set. The global approach using the superposed constraint forces faces difficulty in detecting the local damage under the existence of external noise, because the noise also acts as an external force. The entire structural matrix is decomposed into a matrix representation of the connectivity between the boundary DOFs. The constraint forces dissolved by the elements help in detecting the damage. This is a disassembling-based approach.

Figure 1(a) shows the deflection curves of a simply supported beam subjected to a concentrated load P at node $r+1$ before and after the damage. The difference can be reimbursed by the action of an entire force set at all measured nodes.

The beam is modeled as n elements and $(n+1)$ nodes. In Figure 1, the deflection $\widehat{\delta}_i\,(i=2,3,\ldots,n)$ at the intact state is changed as much as the deflection $\Delta\delta_i\,(i=2,3,\ldots,n)$ at node $i\,(i=2,3,\ldots,n)$ owing to the damage at element ④. This study neglects the measurement of the slope DOFs because it is difficult to measure them. Assuming that the vertical displacements at all nodes are measured, the relationships between the forces and displacement variations at all nodes can be established by

$$\begin{aligned}
\Delta F_2 &= \sum_{j=1}^{n} k_{2j}\left(\Delta\delta_j\right),\\
&\vdots\\
\Delta F_i &= \sum_{j=1}^{n} k_{ij}\left(\Delta\delta_j\right),\\
&\vdots\\
\Delta F_n &= \sum_{j=1}^{n} k_{nj}\left(\Delta\delta_j\right),
\end{aligned} \tag{1}$$

where k_{nj} indicates the force at DOF n owing to a unit displacement at DOF j with all other displacement DOFs equal to zero. $\Delta\delta_i$ and ΔF_i denote the displacement variation at DOF i and the corresponding force, respectively. The deflected curve at the damaged state can be estimated by replacing the force set in Figure 1(b).

The force, or displacement variation, is calculated by solving the simultaneous equations presented in equation (1) and by using the Maxwell–Betti reciprocal theorem. The force and displacement variations at all DOFs and the corresponding internal stress or strain in the elements are interdependently determined. The ultimately predicted stress or strain variations contribute little to tracing the locally damaged elements, because their magnitudes calculated from the entire measurement data along all admissible paths cannot be compared.

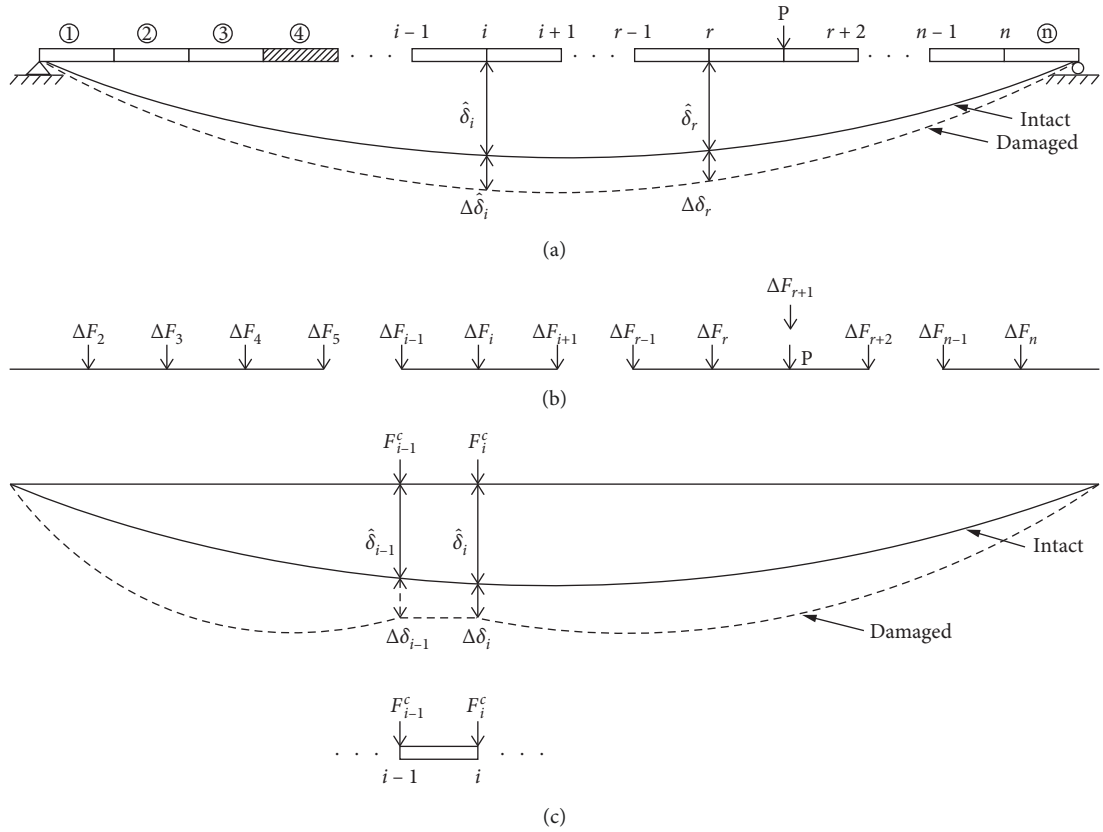

Figure 1: Deflection of a simply supported beam of (a) deflected curves, (b) a force set required for describing the displacement variations, and (c) constraint forces at nodes of a local element i.

Recognizing larger displacement differences or constraint forces at the damaged element, this study disassembles the entire structure into elements. The isolated elements and the correspondingly measured displacements are utilized for predicting the constraint forces. The internal stress calculated from the measured displacements at the boundary DOFs of each element is compared with the stress at the intact state. The damaged element can be detected and is utilized as the damage index for the local approach.

The local approach in this study disassembles an entire structure and considers elements with the measured responses. By estimating the constraint forces at the boundary DOFs of the isolated element ① in Figure 1(c), the internal stresses at both states can be compared and the damaged elements can be detected. The constraint forces are calculated based on the displacements at nodes $(i-1)$ and i without any consideration of the displacement coincidence at the other DOFs. The constraint forces and the constrained equilibrium equation are derived as follows.

The equilibrium equation for an entire structure or substructure with l DOFs can be written as

$$\mathbf{F} = \mathbf{K}\hat{\mathbf{u}}, \tag{2}$$

where $\mathbf{K}$ is the $l \times l$ stiffness matrix and $\mathbf{F}$ and $\hat{\mathbf{u}}$ denote the $l \times 1$ external force vector and displacement vector at the intact state, respectively.

The measurement data in equation (2) at the damaged state can be regarded as constraints to govern the damaged behavior. Assuming that $m\,(l > m)$ data are measured on the boundary of the model, they can be written as

$$\mathbf{A}\mathbf{u} = \mathbf{b}, \tag{3}$$

where $\mathbf{A}$ is the $m \times l$ Boolean matrix for defining the measurement DOFs, $\mathbf{u}$ is the $n \times 1$ constrained response vector, and $\mathbf{b}$ is the $m \times 1$ measured displacement vector.

Combining equations (2) and (3), the constrained equilibrium equation and the constraint force vector $\mathbf{F}^c$ are, respectively, derived [9] by

$$\mathbf{u} = \hat{\mathbf{u}} + \mathbf{K}^{-1/2}\left(\mathbf{A}\mathbf{K}^{-1/2}\right)^{+}(\mathbf{b} - \mathbf{A}\hat{\mathbf{u}}), \tag{4}$$

$$\mathbf{F}^c = \mathbf{K}^{1/2}\left(\mathbf{A}\mathbf{K}^{-1/2}\right)^{+}(\mathbf{b} - \mathbf{A}\hat{\mathbf{u}}), \tag{5}$$

where the second term on the right-hand side of equation (4) represents the displacement variations owing to causes such as damage and construction error. $\mathbf{K}^{-1/2}(\mathbf{A}\mathbf{K}^{-1/2})^{+}$ denotes the weighting matrix.

The constraint forces used to multiply the second term on the right-hand side of equation (4) by the stiffness matrix $\mathbf{K}$ are defined as the forces for compensating the displacement variations. It can be predicted that the magnitude of the constraint forces and the corresponding internal stresses

increase with the response difference $(\mathbf{b} - \mathbf{A}\widehat{u})$. This study detects the damage from the stress variations in the disassembled elements in the elastic range between both states.

3. Example 1

Truss structures are composed of individual structural members to carry tension or compression forces. Each member is modeled as a finite element. The validity of the disassembling-based damage detection method is illustrated through a numerical example of the plane truss structure shown in Figure 2. In the figure, the nodal points and members are numbered. Each node has two DOFs of the horizontal and vertical responses u and v, respectively. The truss is composed of six nodes, nine members, and nine DOFs, excluding the boundary DOFs. All members have the same elastic modulus of 200 GPa and cross-sectional area of $2.5 \times 10^{-3}\ \mathrm{m}^2$. The simply supported truss has a single span. Its length is 12 m, its height is 3 m, and each bay is 4 m long. The responses at the intact state can be calculated by the finite-element method under the action of an external force of 6 kN in the downward direction of node 4. The elemental stiffness matrices and responses at the intact state should be saved for subsequent analysis.

Table 1 lists the measured displacement DOFs corresponding to the disassembled elements. The health state at element ⑤ is investigated using displacements u_3, v_3, u_4, and v_4 at nodes 3 and 4. The constraint forces and internal stresses are calculated using the displacement data measured at the corresponding DOFs.

The damage is established as 20% section loss. The damage detection of a plane truss structure model with single and multiple damaged elements is considered. A single damage case with damage at vertical member ③ or a lower chord ④ and the multiple damage case with damage at a lower chord member ④ and a vertical member ⑦ are considered. The vertical member ③ must be a zero-force member at the intact state. The internal stress in this member is caused by the damage or external noise.

The stress variation rate α, defined as the stress variation with respect to the stress of an element at the damaged state, can be calculated by

$$\alpha = \frac{\sigma_{\mathrm{d}} - \sigma_{\mathrm{u}}}{\sigma_{\mathrm{d}}} \times 100\,(\%), \tag{6}$$

where σ_{u} and σ_{d} denote the axial stresses at the undamaged and damaged states, respectively. Moreover, σ_{d} is calculated using the cross-sectional area at the intact state.

This example also evaluates the noise sensitivity of the proposed method. The simulated or measurement dataset $\mathbf{u}$ is established as

$$\mathbf{u} = \mathbf{u}_0\,(1 + \beta\xi), \tag{7}$$

where β denotes the relative magnitude of the error and ξ is a random number variant in the range $[-1,\ 1]$. $\mathbf{u}_0$ is the noise-free dataset.

Figures 3–5 show the numerical results for detecting the damage of the truss structure using the global approach. Figure 3 shows the absolute value of stress difference (ASD) and stress change rate of equation (6) before and after the 20% section loss at element ④. The stresses at both states are estimated by the global approach using the numerically simulated responses at the entire DOFs. It is shown that the damaged element can be explicitly found in the ASD plots of Figures 3(a) and 3(c) regardless of the noise existence. The vertical member ③ should be a zero-force member under the action of external load at node 4. The member carries the force owing to the small magnitude of truncated errors contained in the measured displacements and exhibits a small stress variation rate, as shown in Figure 3(b). Figure 3(d) shows that the stress change rate abruptly increases at vertical members ③ and ⑦ because of the insignificant stresses at the damaged state. The stress variation rate at member ③ is excluded because of the very huge value. Thus, the damage should be detected by the ASD plot only.

Figure 4 shows the ASD and stress variation rate plots using the 5% noise-contaminated displacements when the damage is located at vertical element ③. The plots rarely provide explicit information on the damage. The ASD at element ③ originates from the truncated numerical values. The rate at element ③ is excluded in Figure 4(b) because it displays a huge value. The abrupt change rate is shown at vertical element ⑦ and indicates that the global approach has a limitation in detecting the damage of vertical members because of their insignificant stresses.

Figure 5 shows the stress variation on the detection of multiple damages at lower chord ④ and vertical member ⑦ using the global approach. The numerical results of the noise-free case in Figures 5(a) and 5(b) indicate the damage at elements ④ and ⑦ except the vertical member ③. The global approach can rarely detect the damage in using the noise-contaminated data, as shown in Figures 5(c) and 5(d). The stress change rate at vertical member ③ is excluded in Figure 5(d) because it is a large value.

Figures 6 and 7 consider the detection of single and multiple damages, respectively, and provide the numerical results calculated from the constraint forces at the boundary of the disassembled elements. The local damage is evaluated based on the proposed method by using elements. Figure 6 shows the ASD and stress variation plots of disassembled elements when the damage is located at element ③. External noise acts as the external force to deform the structure. The plots in Figure 6 show that the damage exists at a disassembled element ③ despite the 5% noise-contaminated displacements. The element ③ of zero stress at the intact state indicates the damage, and the 100% stress variation rate at this element indicates the stress increment owing to the damage. Figure 7 shows the ASD and stress variation rate in the truss structure with multiple damages at elements ④ and ⑦. Damage is expected to occur at elements ④ and ⑦ in Figure 7(a). The ASD at element ③ is zero, and its stress rate of 100% should be the stress increment owing to the existence of external noise. The variation is not related to the damage at element ③. It is found that the damages caused by the proposed disassembling method can be explicitly detected by evaluating both the ASD and stress variation rate despite the external noise. The following example investigates the sensitivity of

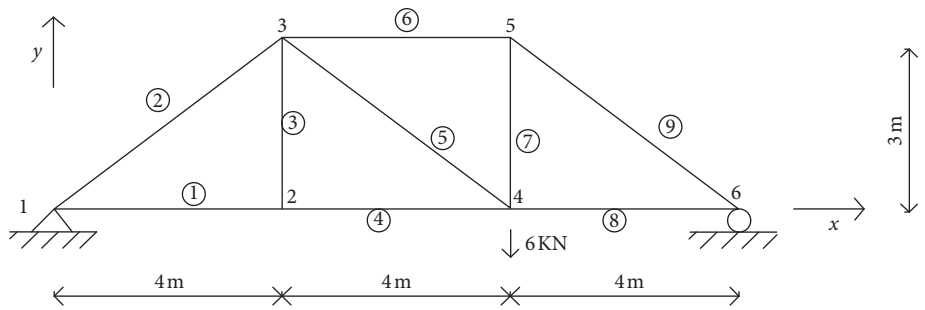

Figure 2: A three-bay truss structure.

Table 1: Disassembled elements and the corresponding DOFs.

Element	①	②	③	④	⑤	⑥	⑦	⑧	⑨
Measured DOFs	u_2	u_3, v_3	v_2, v_3	u_2, u_4	u_3, v_3, u_4, v_4	u_3, u_5	v_4, v_5	u_4, u_6	u_5, v_5, u_6

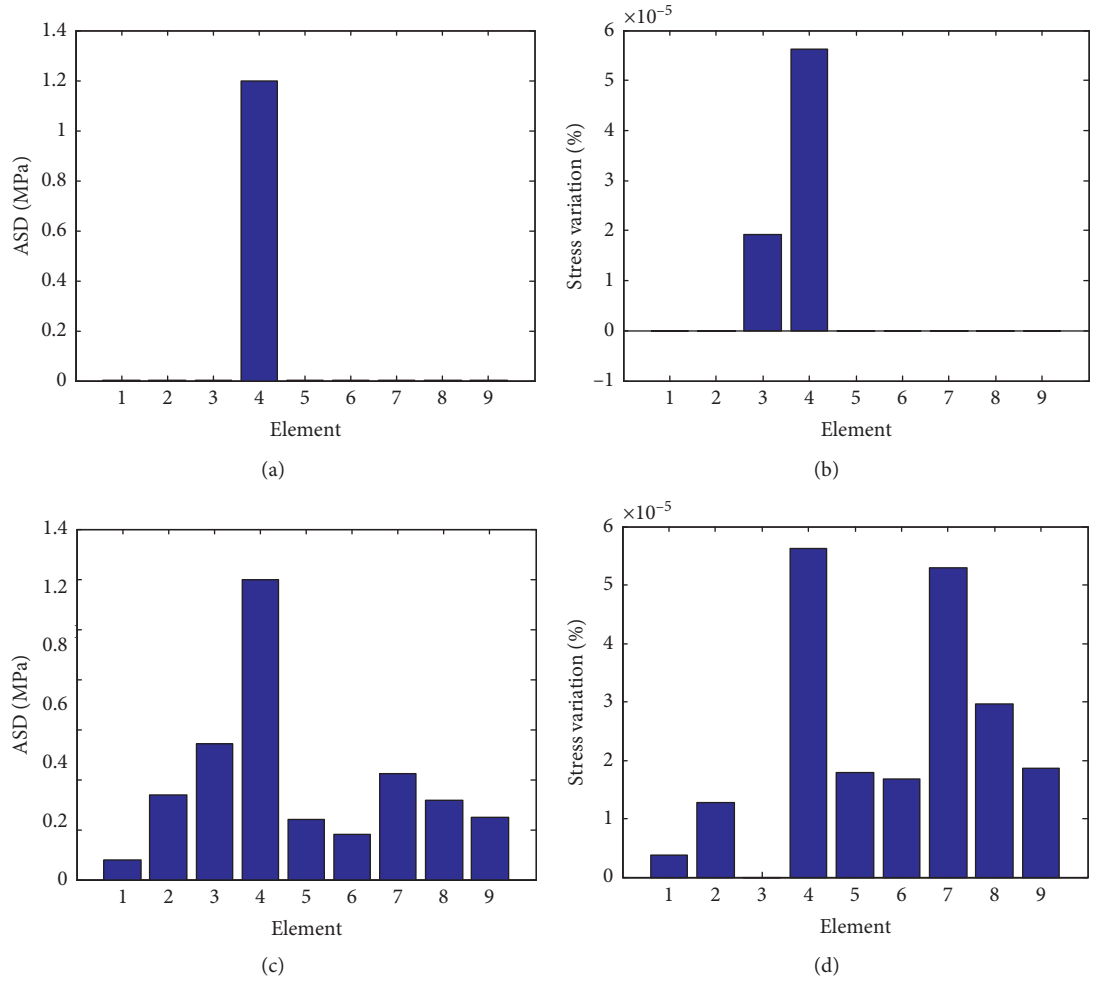

Figure 3: A single damage at element ④ using the global-based approach of (a) ASD of noise-free, (b) stress change rate of noise-free, (c) ASD of 5% noise, and (d) stress change rate of 5% noise.

the local approach depending on the damaged members such as vertical member, diagonal member, and upper and lower chords.

Consider the damage detection of a truss structure composed of 14 nodes and 30 members, as shown in Figure 8. The nodal points and members are numbered. The

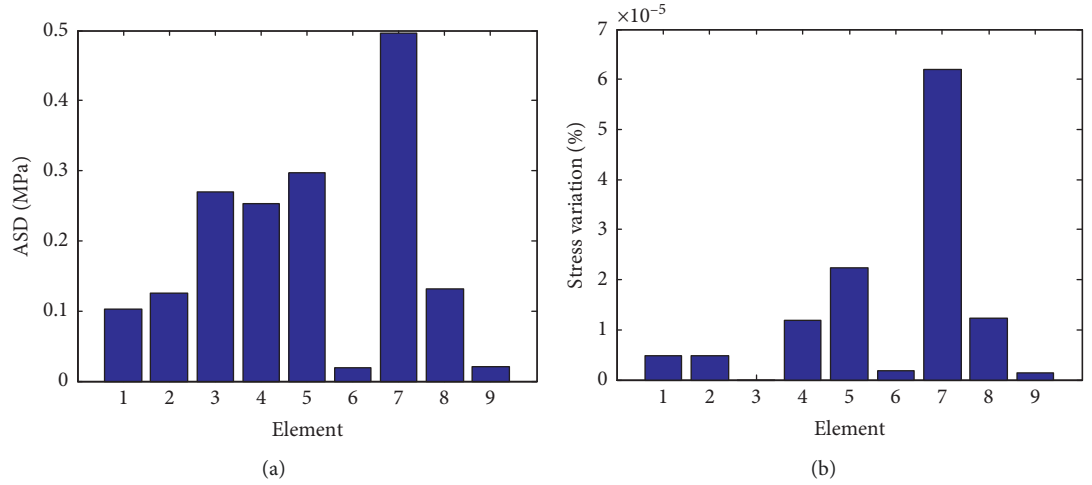

Figure 4: A single damage at element ③ using 5% noise displacements using the global-based approach of (a) ASD and (b) stress change rate.

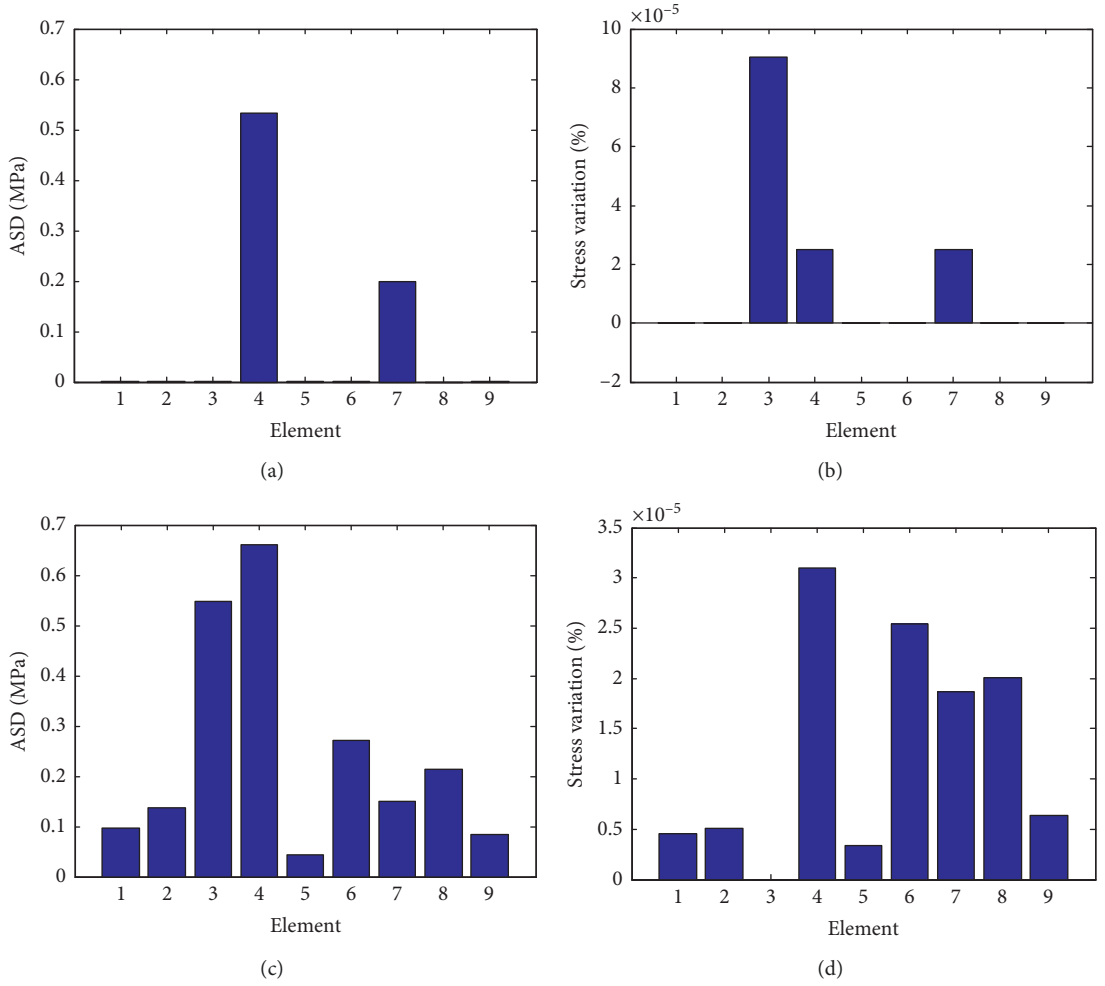

Figure 5: Multiple damages at elements ④ and ⑦ using the global-based approach of (a) ASD of noise-free, (b) stress change rate of noise-free, (c) ASD of 5% noise, and (d) stress change rate of 5% noise.

31 bar truss structure studied by Yang and Sun [11] is considered. All members have the same elastic modulus of 200 GPa, cross-sectional area of 4.0×10^{-3} m^2, and density of 7,800 kg/m^3. The length of a single span truss is 6 m, its height is 1 m, and each bay is 1 m long. It is simply supported with its two translational DOFs at all nodes. A

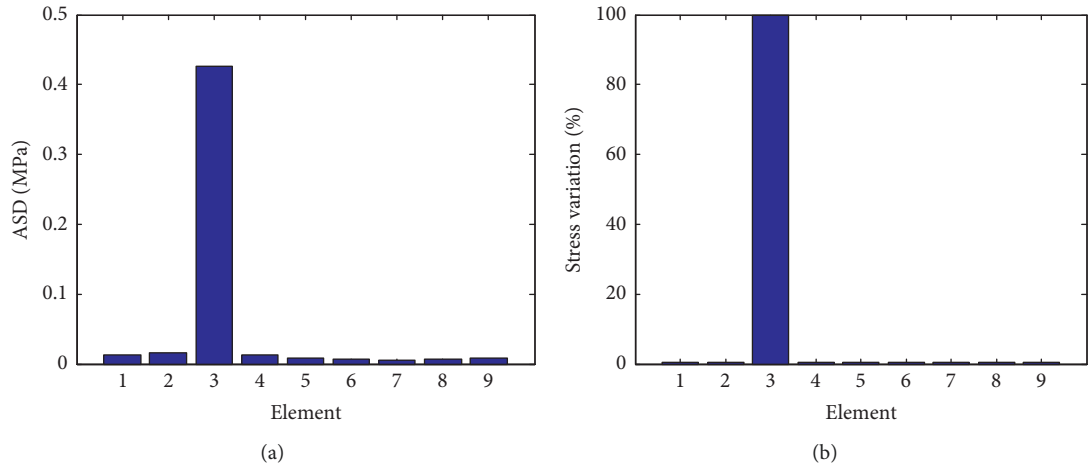

Figure 6: A single damage at element ③ using 5% noise-contaminated measurements and the disassembling-based approach of (a) ASD and (b) stress variation rate.

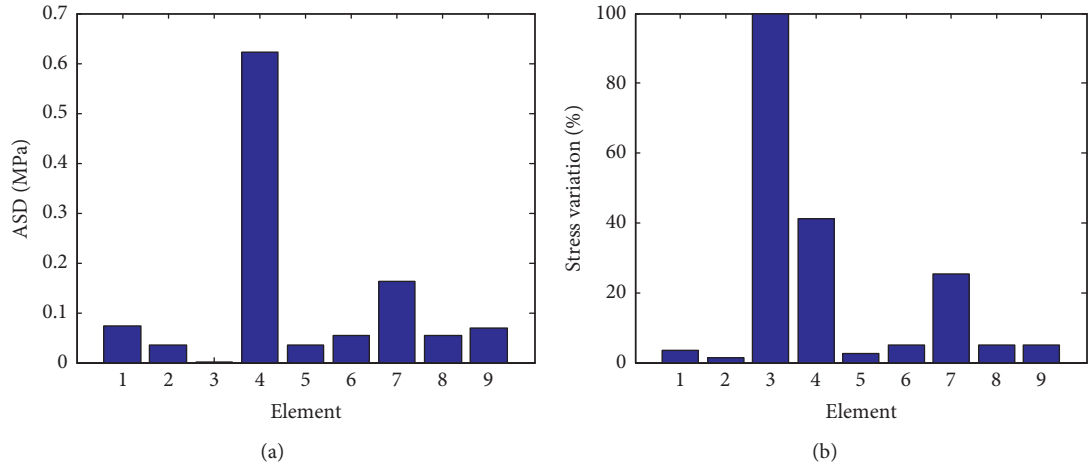

Figure 7: Multiple damages at elements ④ and ⑦ using 5% noise-contaminated measurements and the disassembling-based approach of (a) ASD and (b) stress variation rate.

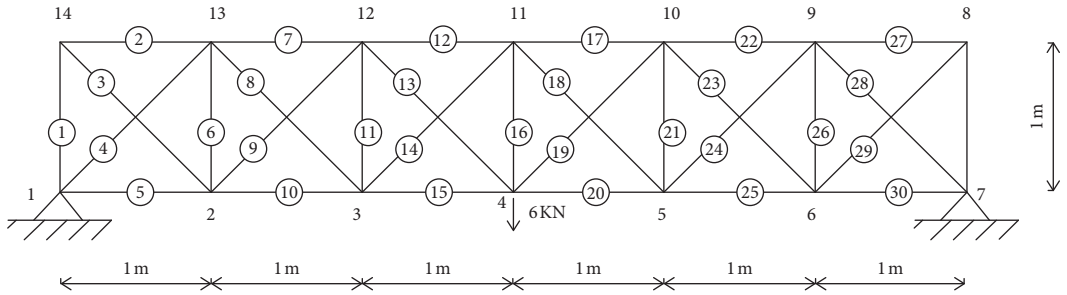

Figure 8: A six bay plane truss structure.

concentrated force of 6 kN acts in the downward direction at node 4.

The numerical results compare the global and local methods for detecting single and multiple damages at vertical, diagonal, and chord members, and the effect of external noise is evaluated. Figure 9 shows the stress difference to be extracted from the noise-free measurement data in the damage of 20% section loss at diagonal member ⑱ using the global approach. The damage is explicitly detected from the ASD plot in Figure 9(a). However, the stress variation rate using equation (6) indicates the damage at the unexpected elements, such as the vertical members in Figure 9(b), because the stresses of the vertical members are calculated by negligible truncated errors. Neglecting the stress variation

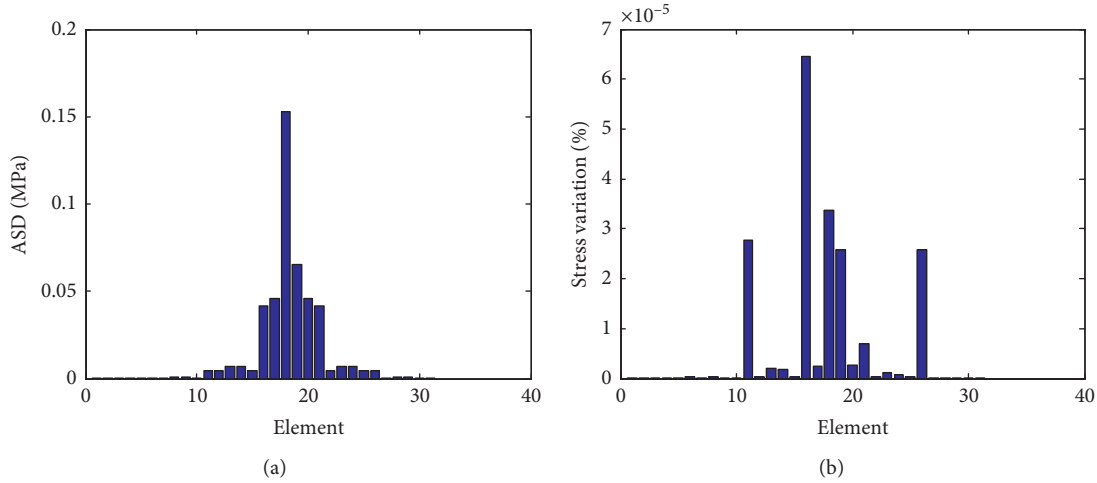

Figure 9: A single damage at element ⑱ using noise-free displacements and global-based approach of (a) ASD and (b) stress variation rate.

rates of the vertical members, the damage can be explicitly detected by analyzing both ASD plots.

Figure 10 shows the stress variation of all members derived using 3% noise-contaminated responses and the global approach. The damage is located at diagonal member ⑱. It is observed that the stresses predicted by the global approach are very sensitive to the external noise, and hence, the damage cannot be detected. The stress variation rate abruptly increases at the vertical members because of the insignificant stress at the damaged state.

Figure 11 shows the stress variations using the disassembling-based damage detection approach. The damage of 20% section loss is located at diagonal element ⑱, and the 3% noise-contaminated responses at the DOFs of u_5, v_5, u_{11}, and v_{11} are utilized as the measurements. The damaged element can be explicitly detected by the ASD plot in Figure 11(a). Considering that the abrupt change in the stress variation rate at vertical members ⑪, ⑯, and ㉖ in Figure 11(b) originates from the insignificant stress at the damage state, they are excluded from the damage-expected elements. This indicates that the proposed method can be utilized in detecting the locally damaged member along the load path on an isolated element. The noise is revealed to the external forces to act on a full set of DOFs and is carried along various load paths. The damage can be found when the specific load path coincides with the path along the damaged member. Thus, the damage can be more explicitly detected in utilizing the local approach rather than the global approach.

Figure 12 shows the numerical results of the proposed disassembling-based method to detect multiple damages of 20% section loss at diagonal members ⑨ and ⑱. It is found that the damage can rarely be detected by the stress change rate in Figure 12(b) because of the abrupt stress change at the vertical members. The ASD plot in Figure 12(a) shows an abrupt change at the damaged members in noise-free case and provides enough damage information. The noise effect is shown in Figure 13. The fluctuating change in the ASD is observed in the presence of 2% external noise compared to the noise-free case. This indicates that the method is slightly affected by external noise as compared to the single damage case at element ⑱ in Figure 11(a), but the damaged members are explicitly detected.

Figure 14 shows the numerical results of damage detection at the upper and lower members of ⑩ and ⑰ using 3% noise-contaminated responses and the local approach. The damaged members are explicitly detected despite the external noise, showing that the chord members corresponding to the compression and tension regions of the beam member can be more explicitly detected unlike the diagonal and vertical members.

Figures 15 and 16 show the stress variations predicted by the global damage detection method of the truss structure with damages of 20% section loss at vertical member ㉖, upper chord ⑩, and diagonal member ⑰. The ASD plot in the noise-free case explicitly indicates the damage of the diagonal member and the upper chord, except at vertical member ㉖, as shown in Figure 15(a). The damages at the vertical members are presumed by the stress variation rate in Figure 15(b). It is observed that the stress variation rate has difficulty in detecting the damage of the vertical member. The noise effect contained in the measured responses data is investigated as shown in Figure 16, and the ASD plot in Figure 16(a) shows that the global method is very sensitive to external noise and can be rarely utilized in detecting the damage. The stress variation rate in the vertical members is not related to the damage, and it does not help detect the damage.

The numerical results obtained using the local approach proposed in this study are shown in Figures 17 and 18. This case considers damage detection at the same members as those shown in Figure 16. In the noise-free case as shown by Figure 17, the plots exhibit a similar tendency as that observed in the previous global approach. However, both plots of the ASD and stress change rate obtained by the local approach provide evidence to detect the damage at vertical member ㉖ unlike the global approach. The damage at vertical member ㉖ can be detected. In the 3% noise-

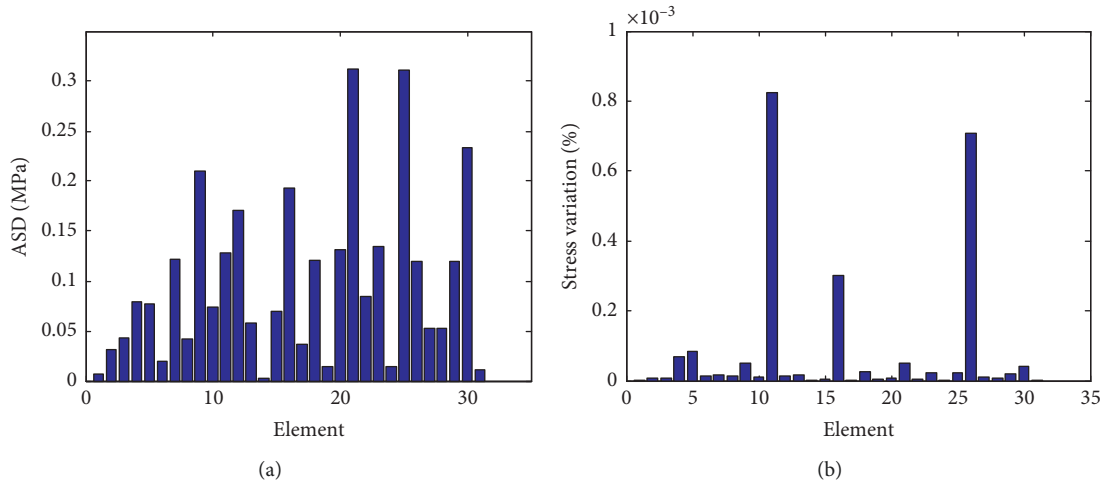

Figure 10: A single damage at element (18) using 3% noise-contaminated displacements and global-based approach of (a) ASD and (b) stress variation rate.

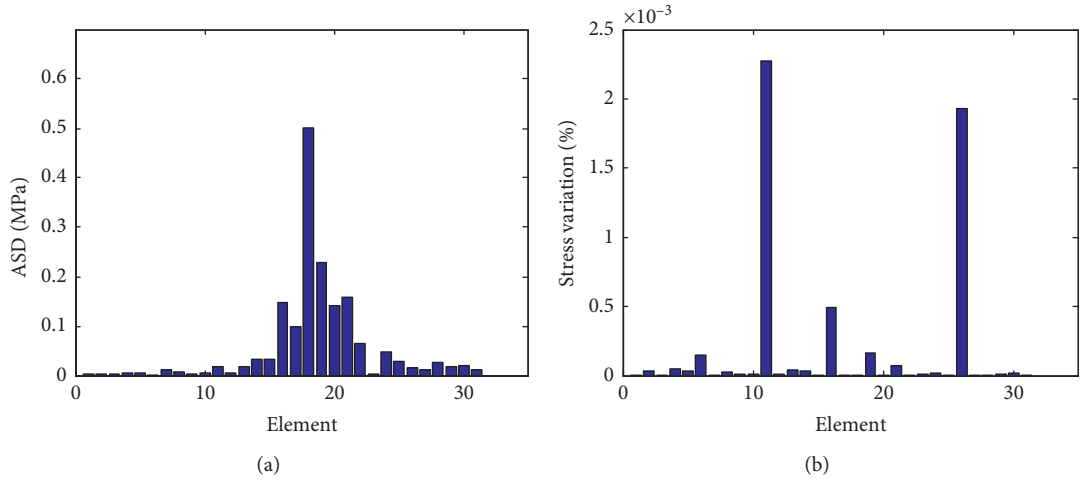

Figure 11: A single damage at element (18) using 3% noise displacements and local-based approach of (a) ASD and (b) stress variation rate.

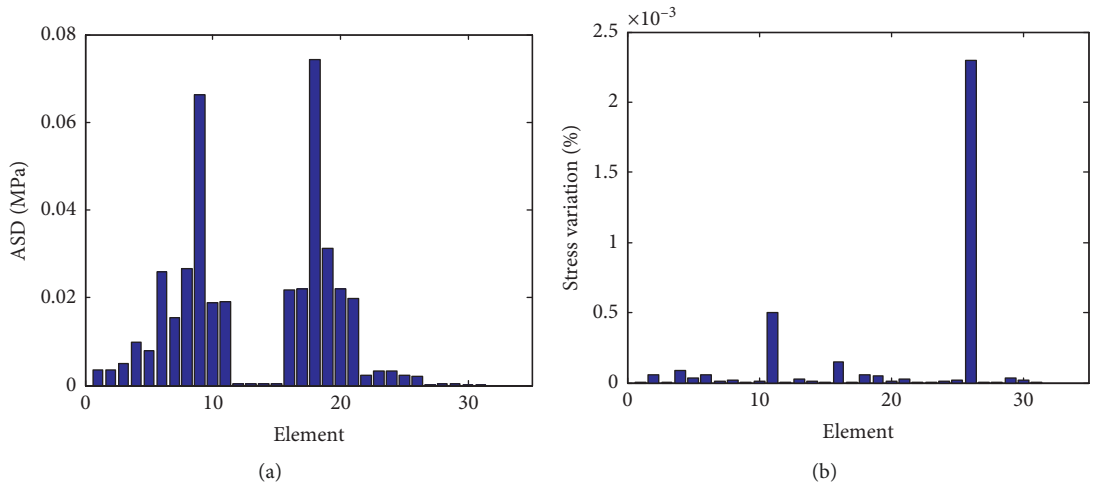

Figure 12: Multiple damages at elements (9) and (18) using noise-free displacements and local-based approach of (a) ASD and (b) stress variation rate.

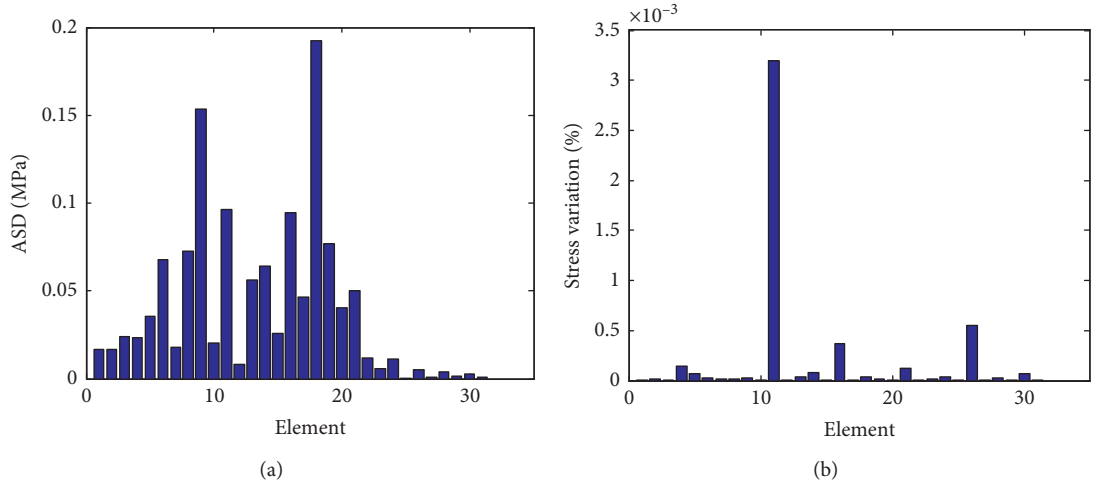

Figure 13: Multiple damages at elements ⑨ and ⑱ using 2% noise-contaminated displacements of (a) ASD and (b) stress variation rate.

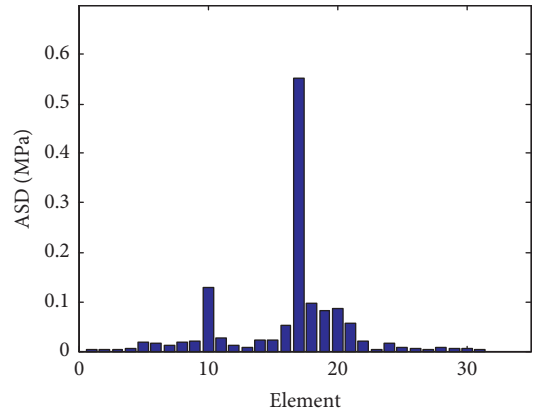

Figure 14: ASD of the truss with multiple damages at elements ⑩ and ⑰ using 3% noise-contaminated displacements and local-based approach.

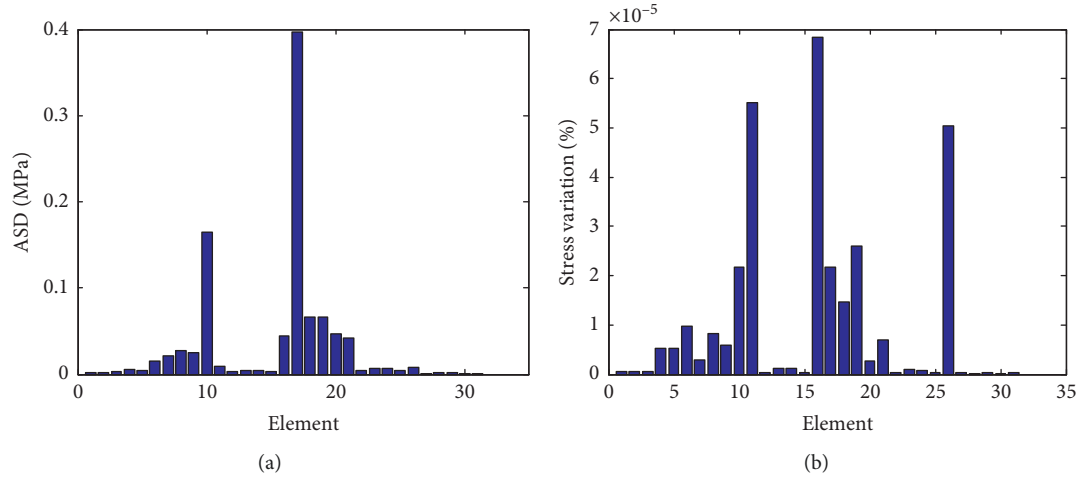

Figure 15: Multiple damages at elements ⑩, ⑰, and ㉖ using noise-free displacements and global-based approach of (a) ASD and (b) stress variation rate.

contaminated case shown by Figure 18, the damaged members can be explicitly detected by ASD and stress change rate despite the external noise. It can be concluded that the local-based approach considering the noise effect can be more explicitly utilized in detecting the damage of the structural members, as compared to the global approach.

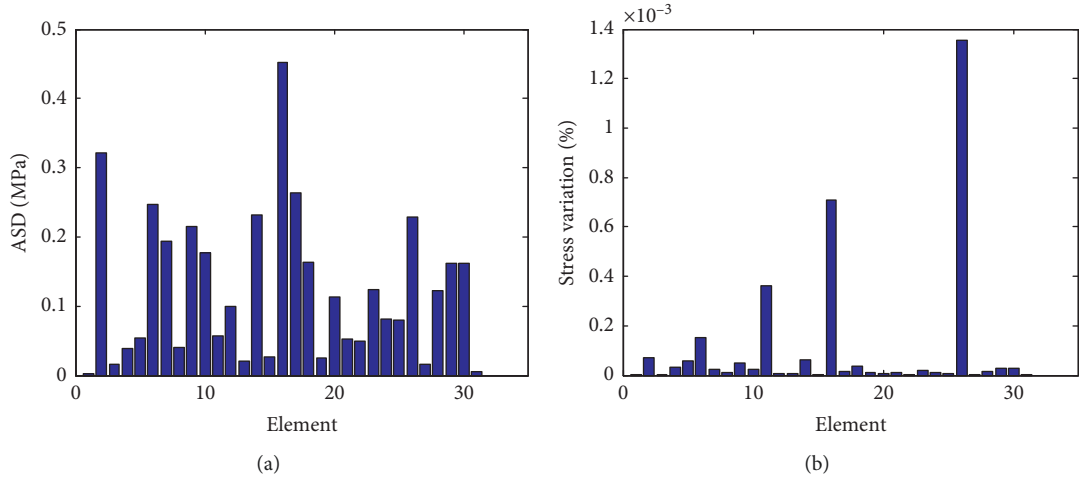

Figure 16: Multiple damages at elements ⑩, ⑰, and ㉖ using 3% noise-contaminated displacements and global-based approach of (a) ASD and (b) stress variation rate.

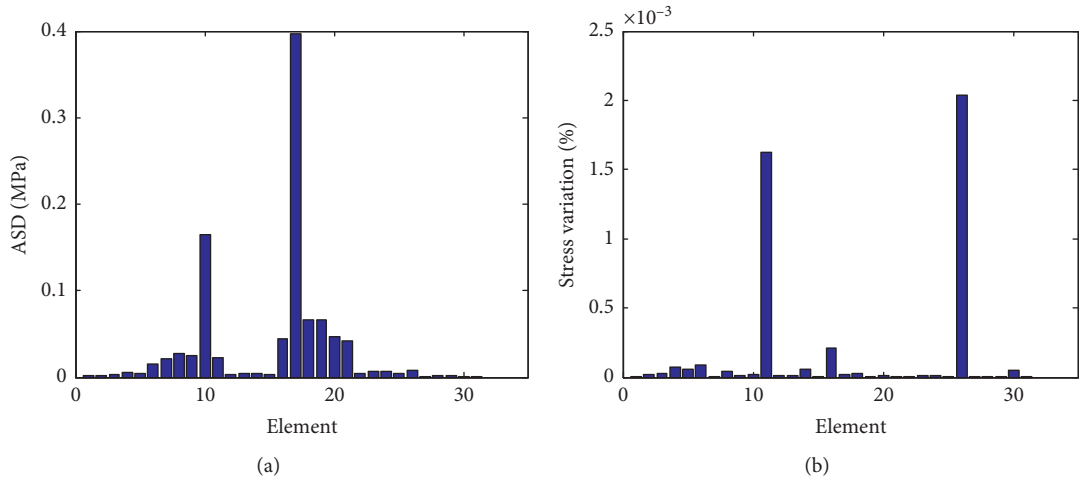

Figure 17: Multiple damages at elements ⑩, ⑰, and ㉖ using noise-free displacements and local-based approach of (a) ASD and (b) stress variation rate.

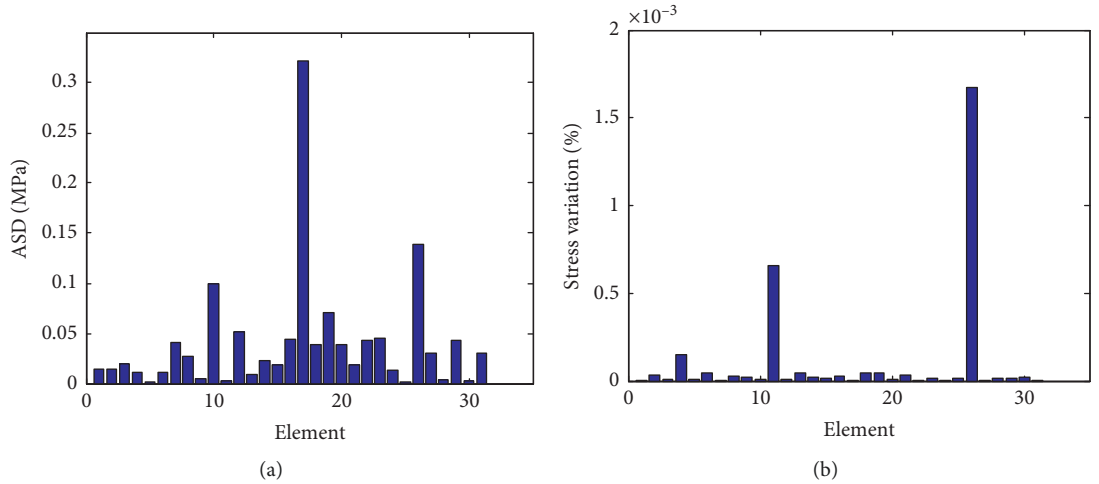

Figure 18: Multiple damages at elements ⑩, ⑰, and ㉖ using 3% noise and local-based approach of (a) ASD and (b) stress variation rate.

4. Conclusions

This paper presents a local damage detection method disassembling an entire structure into finite elements and using the measured static responses. The measured responses are transformed to the constraint forces and internal stresses at the presumed elements or substructures, and the damage is detected by the stress variations before and after the damage. It is shown that the local approach can be utilized as a more explicit damage detection method than the global approach. The damage is detected by the local approach when it is located along the load path. The validity of the proposed disassembling-based approach is illustrated through the damage detection of two truss structures. It is concluded that the proposed method can be explicitly utilized in detecting the damage despite the external noise.

Data Availability

The numerical data used to support the findings of this study are included within the article.

Conflicts of Interest

The authors declare that they have no conflicts of interest.

Acknowledgments

This research was supported by Basic Science Research Program through the National Research Foundation of Korea (NRF) funded by the Ministry of Education (NRF-2016R1D1A1A09918011). This study was supported by the 2017 Research Grant Kangwon National University (No. 520170128).

References

[1] X.-Z. Chen, Z. Hong-Ping, and C. Chuan-Yao, "Structural damage identification using test static data based on grey system theory," *Journal of Zhejiang University-SCIENCE A*, vol. 6, no. 8, pp. 790–796, 2005.

[2] S. W. Doebling, L. D. Peterson, and K. F. Alvin, "Experimental determination of local structural stiffness by disassembly of measured flexibility matrices," *Journal of Vibration and Acoustics*, vol. 120, no. 4, pp. 949–957, 1998.

[3] S. W. Doebling, *Damage Detection and Model Refinement Using Elemental Stiffness Perturbations with Constrained Connectivity*, AIAA, Reston, VA, USA, 1996.

[4] G. James, T. Cao, M. Kaouk, and D. Zimmerman, "A coupled approach for structural damage detection with incomplete measurements," in *Conference Proceedings of the Society for Experimental Mechanics Series*, Springer, New York, NY, USA, 2014.

[5] M. Montazer and S. M. Seyedpoor, "A new flexibility based damage index for damage detection of truss structures," *Shock and Vibration*, vol. 2014, Article ID 460692, 12 pages, 2014.

[6] F. Bakhtiari-Nejad, A. Rahai, and A. Esfandiari, "A structural damage detection method using static noisy data," *Engineering Structures*, vol. 27, no. 12, pp. 1784–1793, 2005.

[7] D. Maity and A. Saha, "Damage assessment in structure from changes in static parameter using neural networks," *Sadhana*, vol. 29, no. 3, pp. 315–327, 2004.

[8] M. Rezaiee-Pajand, M. S. Kazemiyan, and A. S. Aftabi, "Static damage identification of 3D and 2D frames," *Mechanics Based Design of Structures and Machines*, vol. 42, no. 1, pp. 70–96, 2014.

[9] S. Rahmatalla, E.-T. Lee, and H.-C. Eun, "Damage detection by the distribution of predicted constraint forces," *Journal of Mechanical Science and Technology*, vol. 26, no. 4, pp. 1079–1087, 2012.

[10] Q. W. Yang, "A numerical technique for structural damage detection," *Applied Mathematics and Computation*, vol. 215, no. 7, pp. 2775–2780, 2009.

[11] Q. W. Yang and B. X. Sun, "Structural damage localization and quantification using static test data," *Structural Health Monitoring: An International Journal*, vol. 10, no. 4, pp. 381–389, 2010.

[12] K. D. Hejelmstad and S. Shin, "Damage detection and assessment of structures from static response," *Journal of Engineering Mechanics*, vol. 123, no. 6, pp. 568–576, 1997.